

1-1-2016

A carbonate-based proxy for sulfate-driven anaerobic oxidation of methane

Dong Feng

South China Seas Institute of Oceanography Chinese Academy of Sciences

Yongbo Peng

Louisiana State University

Huiming Bao

Louisiana State University

Jörn Peckmann

Universität Hamburg

Harry H. Roberts

Louisiana State University

See next page for additional authors

Follow this and additional works at: https://repository.lsu.edu/geo_pubs

Recommended Citation

Feng, D., Peng, Y., Bao, H., Peckmann, J., Roberts, H., & Chen, D. (2016). A carbonate-based proxy for sulfate-driven anaerobic oxidation of methane. *Geology*, 44 (12), 999-1002. <https://doi.org/10.1130/G38233.1>

This Article is brought to you for free and open access by the Department of Geology and Geophysics at LSU Scholarly Repository. It has been accepted for inclusion in Faculty Publications by an authorized administrator of LSU Scholarly Repository. For more information, please contact ir@lsu.edu.

Authors

Dong Feng, Yongbo Peng, Huiming Bao, Jörn Peckmann, Harry H. Roberts, and Duofu Chen

A carbonate-based proxy for sulfate-driven anaerobic oxidation of methane

Dong Feng^{1*}, Yongbo Peng^{2*}, Huiming Bao², Jörn Peckmann^{3,4}, Harry H. Roberts⁵, and Duofu Chen⁶

¹Key Laboratory of Marginal Sea Geology, South China Sea Institute of Oceanology, Chinese Academy of Sciences, Guangzhou 510301, China

²Department of Geology and Geophysics, Louisiana State University, Baton Rouge, Louisiana 70803, USA

³Institute of Geology, University of Hamburg, 20146 Hamburg, Germany

⁴Department of Geodynamics and Sedimentology, University of Vienna, 1090 Vienna, Austria

⁵Coastal Studies Institute, Department of Oceanography and Coastal Sciences, Louisiana State University, Baton Rouge, Louisiana 70803, USA

⁶Shanghai Engineering Research Center of Hadal Science and Technology, College of Marine Sciences, Shanghai Ocean University, Shanghai 201306, China

ABSTRACT

Sulfate-driven anaerobic oxidation of methane (SD-AOM) supports chemosynthesis-based communities and limits the release of methane from marine sediments. Formation of authigenic carbonates at active methane seeps is promoted by SD-AOM stoichiometry. While distinctively small $\delta^{18}\text{O}/\delta^{34}\text{S}$ slopes of pore fluid sulfate have been shown to typify modern methane-rich environments, identification of such environments has been difficult for the geological past due to the lack of sedimentary pore fluids. However, if the isotopic composition of sulfate were archived in authigenic carbonate during early diagenesis, carbonate-associated sulfate (CAS) should display the characteristic $\delta^{18}\text{O}-\delta^{34}\text{S}$ pattern. To test this hypothesis, we investigated the $\delta^{18}\text{O}_{\text{CAS}}$, $\delta^{34}\text{S}_{\text{CAS}}$, and $^{87}\text{Sr}/^{86}\text{Sr}$ signatures of authigenic carbonate minerals from three modern and two ancient methane-seep provinces. The data obtained demonstrate that all deposits regardless of age or location display consistently small $\delta^{18}\text{O}_{\text{CAS}}/\delta^{34}\text{S}_{\text{CAS}}$ slopes (~ 0.3) and CAS does not represent ambient seawater but pore-water sulfate. This finding confirms the utility of CAS as a recorder of SD-AOM in methane-rich environments. In addition, we report that aragonites bear higher CAS contents, $^{87}\text{Sr}/^{86}\text{Sr}$ ratios closer to that of contemporary seawater, and a larger $\delta^{18}\text{O}_{\text{CAS}}/\delta^{34}\text{S}_{\text{CAS}}$ slope than calcites, reflecting the shallower formation depth of aragonite where pore-water has a composition close to that of seawater with high concentrations of sulfate. The new proxy can be used to constrain the record of SD-AOM through most of Earth history by measuring the $\delta^{18}\text{O}$ and $\delta^{34}\text{S}$ values of CAS of methane-derived diagenetic carbonates including but not limited to seep carbonates.

INTRODUCTION

Sulfate-driven anaerobic oxidation of methane (SD-AOM) has been shown to consume 90% or more of the methane produced in subsurface seafloor environments (e.g., Niewöhner et al., 1998; Knittel and Boetius, 2009). In methane-rich marine sediments, methane oxidation is primarily coupled to sulfate reduction, which is mediated by a consortium of anaerobic methanotrophic archaea and sulfate-reducing bacteria (Boetius et al., 2000). Although other electron acceptors are known to be able to sustain anaerobic oxidation of methane, SD-AOM sustains some of the richest marine ecosystems along modern continental margins at sites referred to as methane seeps (e.g., Boetius and Wenzhöfer, 2013). It has been shown that rates of sulfate reduction in methane-seep sediments can be several orders of magnitude higher than in non-seep sediments

(Aharon and Fu, 2000; Joye et al., 2004). Sulfate, the electron acceptor, can change its concentrations, fluxes, and stable sulfur and oxygen isotope compositions during SD-AOM (Aharon and Fu, 2000; Joye et al., 2004; Bowles et al., 2014). However, SD-AOM processes could have been insignificant in the geological past when sulfate concentration was low (Bristow and Grotzinger, 2013). Thus, a geological record of SD-AOM can provide information on the evolution of Earth's surface environments and specifically the sulfate concentration in paleo-oceans.

Oxygen and sulfur stable isotope compositions of dissolved sulfate ($\delta^{18}\text{O}_{\text{SO}_4}$ and $\delta^{34}\text{S}_{\text{SO}_4}$) in modern sedimentary pore fluids affected by both organotrophic and methanotrophic microbial sulfate reduction have been analyzed to explore the respective operation modes (e.g., Böttcher et al., 1998, 2001; Aharon and Fu, 2000; Antler et al., 2013, 2014, 2015; Deusner et al., 2014; Rennie and Turchyn, 2014). Antler et al. (2015) discovered that SD-AOM in methane-rich environments results in distinctively small $\delta^{18}\text{O}_{\text{SO}_4}/\delta^{34}\text{S}_{\text{SO}_4}$ slopes (0.24–0.4), which differ from the larger slopes typifying organotrophic sulfate reduction or sites of diffusive flux of methane within marine sediments. It has been put forward that barite deposits might be a potential proxy to look into the geological record of AOM (e.g., Böttcher and Parafiniuk, 1998; Torres et al., 2003). However, authigenic barite is relatively sparse in contrast to carbonate at modern seeps and in ancient seep deposits (Peckmann and Thiel, 2004; Campbell, 2006). Authigenic carbonate commonly forms under both methane diffusion-controlled and methane-rich conditions (Luff and Wallmann, 2003), and carbonate minerals can preserve pore-water sulfate as carbonate-associated sulfate (CAS; Staudt and Schoonen, 1995). Methane-seep carbonates have been reported to occur throughout much of Earth history (e.g., Peckmann and Thiel, 2004; Campbell, 2006), and their carbon and oxygen isotope signatures reflect the involvement of methane in sulfate reduction-driven authigenesis.

To examine if the isotopic composition of CAS from seep carbonates indeed reveals a specific, characteristically small $\delta^{18}\text{O}_{\text{SO}_4}/\delta^{34}\text{S}_{\text{SO}_4}$ slope, we conducted a survey of $\delta^{18}\text{O}_{\text{CAS}}-\delta^{34}\text{S}_{\text{CAS}}$ data pairs from three modern (Gulf of Mexico; Black Sea; South China Sea) and two ancient (Neogene, northern Italy; Paleogene, western Washington State, USA) seep provinces (Fig. 1). The focus is on seep carbonates from the Gulf of Mexico where a great number of samples representing different types of seepage were available and the presence of both aragonite and calcite mineralogies allowed for a mineral-specific analysis of CAS composition.

MATERIALS AND METHODS

Authigenic carbonates used for this study have been previously shown to represent marine hydrocarbon-seep deposits (see the GSA Data

*E-mails: feng@scsio.ac.cn; ypeng@lsu.edu

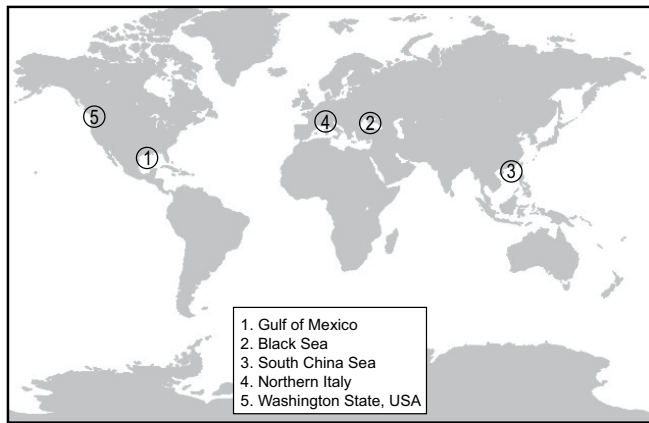


Figure 1. Global map showing five study areas.

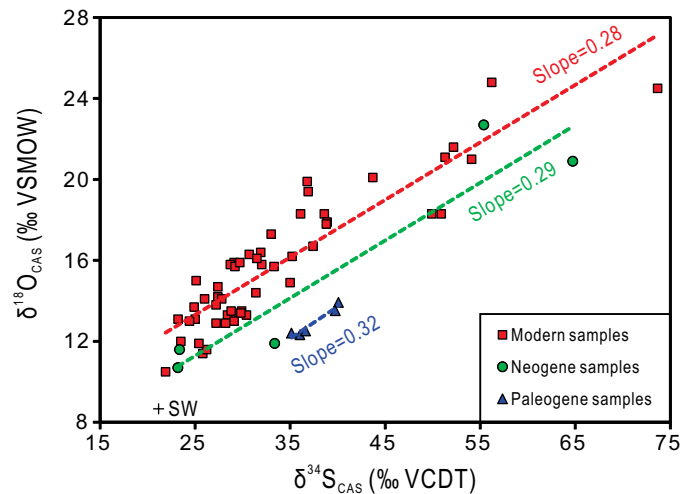


Figure 2. $\delta^{18}\text{O}_{\text{CAS}}$ (CAS—carbonate-associated sulfate) versus $\delta^{34}\text{S}_{\text{CAS}}$ values of seep carbonates from modern seafloor (Gulf of Mexico and Black Sea), Neogene deposits (Northern Italy), and Paleogene deposits (western Washington State, USA). VCDT—Vienna Canyon Diablo troilite; VSMOW—Vienna standard mean ocean water. Black cross corresponds to $\delta^{18}\text{O}$ and $\delta^{34}\text{S}$ composition of modern seawater (SW) sulfate.

Repository¹ for materials). The modern Gulf of Mexico samples are subdivided into two groups based on the dominance of either aragonite or calcite. Clean carbonate samples were analyzed for CAS contents, $\delta^{18}\text{O}_{\text{CAS}}$, $\delta^{34}\text{S}_{\text{CAS}}$, pyrite content, $\delta^{13}\text{C}_{\text{pyrite}}$, $\delta^{18}\text{O}_{\text{carbonate}}$, and $^{87}\text{Sr}/^{86}\text{Sr}_{\text{carbonate}}$ (see the Data Repository for analytical methods). The experimental procedures used ensured that the observed CAS stable isotope patterns represent primary signatures reflecting pore-water sulfate at the respective seep sites.

RESULTS

The overall $\delta^{18}\text{O}_{\text{CAS}}/\delta^{34}\text{S}_{\text{CAS}}$ slopes are more or less parallel among the modern samples (Gulf of Mexico and Black Sea), the Neogene samples, and the Paleogene samples with slopes of 0.28 ($R^2 = 0.81$, $n = 52$), 0.29 ($R^2 = 0.89$, $n = 5$), and 0.32 ($R^2 = 0.94$, $n = 5$), respectively (Fig. 2). On a plot of Gulf of Mexico samples that distinguishes aragonite and calcite mineralogy, the CAS isotope data for aragonite and for calcite have slopes of 0.53 ($R^2 = 0.81$, $n = 12$) and 0.30 ($R^2 = 0.80$, $n = 38$), respectively, with the aragonite array falling on a line with open-ocean seawater sulfate ($\delta^{18}\text{O} = 8.7\text{‰}$ and $\delta^{34}\text{S} = 21.2\text{‰}$; Johnston et al., 2014; Fig. 3), whereas the calcite array projects to higher $\delta^{18}\text{O}$ and $\delta^{34}\text{S}$ values.

The CAS contents in Gulf of Mexico aragonite and calcite vary widely and without an apparent pattern, clustering around averages of 249 ppm (± 145 , 1 standard deviation [SD], $n = 12$) and 188 ppm (± 141 , 1 SD, $n = 38$), respectively (Table DR2 in the Data Repository). The CAS contents of the two Black Sea high-Mg calcites are rather low, ranging from 82 ppm to 93 ppm. Neogene seep carbonates from northern Italy have lower CAS contents than Paleogene seep carbonates from western Washington State, but all fall within the CAS concentration range of the Gulf of Mexico samples.

The $^{87}\text{Sr}/^{86}\text{Sr}$ ratios of 40 samples from the Gulf of Mexico fall between 0.708357 and 0.710214 (Fig. 4). Within this sample set, aragonite samples (0.709154–0.709205) typically display values close to that of modern seawater (0.709175; Fu and Aharon, 1998), whereas calcite samples show a large variation, ranging from 0.708357 to 0.710124.

DISCUSSION

The $\delta^{18}\text{O}_{\text{CAS}}-\delta^{34}\text{S}_{\text{CAS}}$ plots of modern and ancient methane-seep carbonates reveal not only strong correlations, but more importantly, a characteristic slope of ~ 0.3 . This slope is at the lower end of the $\delta^{18}\text{O}/\delta^{34}\text{S}$ slope range (0.29–0.47) observed from pore-water sulfate in modern methane-rich environments and is considerably different from a slope of ≥ 0.4 for

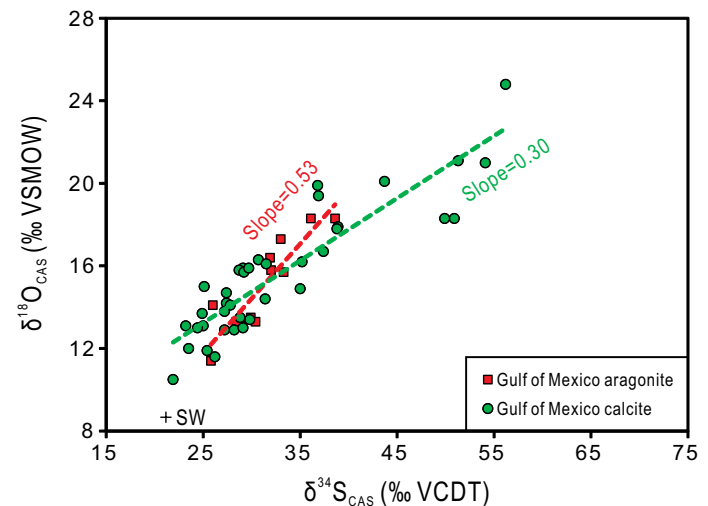


Figure 3. $\delta^{18}\text{O}_{\text{CAS}}$ (CAS—carbonate-associated sulfate) versus $\delta^{34}\text{S}_{\text{CAS}}$ values of Gulf of Mexico seep carbonates grouped by dominant mineral composition (aragonite dominated versus calcite dominated). VCDT—Vienna Canyon Diablo troilite; VSMOW—Vienna standard mean ocean water. Black cross corresponds to $\delta^{18}\text{O}$ and $\delta^{34}\text{S}$ composition of modern seawater (SW) sulfate.

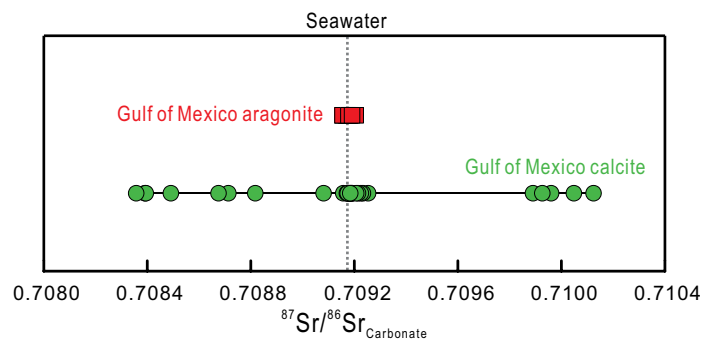


Figure 4. Strontium isotope data for Gulf of Mexico aragonite and calcite. Dashed line corresponds to $^{87}\text{Sr}/^{86}\text{Sr}$ ratio of modern Gulf of Mexico seawater (0.709175; Fu and Aharon, 1998).

¹GSA Data Repository item 2016336, description of samples and analytical methods, results of pyrite-rich samples (Figure DR1 and Table DR1), plot of isotope values of seep and non-seep carbonates (Figure DR2), and summary of geochemical data (Table DR2), is available online at <http://www.geosociety.org/pubs/ft2016.htm> or on request from editing@geosociety.org.

pore-water sulfate in methane diffusion-controlled or methane-devoid environments (cf. Antler et al., 2015). Antler et al. (2015) concluded that the slope is independent of physical parameters in the environment (e.g., temperature, water pressure, salinity, and sulfate concentration), and our results support this conclusion. All types of seep carbonates analyzed in this study, regardless of location or age, exhibit small and constant $\delta^{18}\text{O}_{\text{CAS}}/\delta^{34}\text{S}_{\text{CAS}}$ slopes (0.28–0.32; Fig. 2) with the exception of pure aragonite (0.53; Fig. 3). This observation suggests that the extracted CAS from seep carbonates preserved the primary isotope signals of the pore-water sulfate.

During sulfate reduction, ^{34}S and ^{18}O behave differently. The $\delta^{34}\text{S}_{\text{SO}_4}$ value typically increases as the ^{32}S isotope is distilled into the reduced products and fixed in the form of low-solubility metal sulfides. The $\delta^{18}\text{O}_{\text{SO}_4}$ value increases too but tends to reach oxygen isotope equilibrium with ambient water because intermediate-valence-state sulfur species that are formed during microbial sulfate reduction exchange their oxygen atoms with water (e.g., Fritz et al., 1989; Brunner et al., 2005; Wortmann et al., 2007; Wankel et al., 2014). Numerical models of Antler et al. (2015) confirmed that the slopes of $\delta^{18}\text{O}/\delta^{34}\text{S}$ of pore-water sulfate in methane-rich environments range from 0.24 to 0.4, where up to 12% of the reduced sulfur intermediates is reoxidized to sulfate through intracellular disproportionation of polysulfide intermediates. When the transport of methane is controlled by diffusion, however, the slope of $\delta^{18}\text{O}/\delta^{34}\text{S}$ increases to >0.4 .

At first glance, the studied samples from the three different age groups display parallel arrays. It might be tempting to conclude that each of the arrays points to the corresponding coeval seawater sulfate $\delta^{34}\text{S}$ and $\delta^{18}\text{O}$ composition; however, such an inference could be incorrect. Paleogene seawater sulfate may have had a somewhat different isotope composition than modern seawater sulfate (Wortmann and Paytan, 2012; Algeo et al., 2015), but the difference is unlikely to have been large. A more likely explanation for the parallel arrays is that different seeps have different methane fluxes, which result in variable depth ranges of methane-rich pore fluids. Above those depths, the sediments are methane diffusion limited or even devoid of methane. In environments characterized by active methane seepage where the sulfate-methane transition zone is commonly located close to the sediment-water interface, the $\delta^{18}\text{O}_{\text{SO}_4}$ - $\delta^{34}\text{S}_{\text{SO}_4}$ isotope array will point to the seawater sulfate isotope value. However, when methane-rich conditions terminate at depth, the $\delta^{18}\text{O}_{\text{SO}_4}$ - $\delta^{34}\text{S}_{\text{SO}_4}$ array should point to the isotope composition of sulfate at that particular depth where both the $\delta^{18}\text{O}_{\text{SO}_4}$ and the $\delta^{34}\text{S}_{\text{SO}_4}$ values should be higher than those of coeval seawater. This interpretation is independently supported by the CAS data from aragonite and calcite samples from the Gulf of Mexico, because it is widely accepted that calcite tends to form at greater depth than aragonite at seeps (e.g., Haas et al., 2010; Nöthen and Kasten, 2011). The larger slope of the $\delta^{18}\text{O}_{\text{CAS}}/\delta^{34}\text{S}_{\text{CAS}}$ array of aragonite (0.53) falls on a line with modern seawater sulfate, but the smaller slope of calcite (0.30) does not project into the isotopic composition of seawater sulfate (Fig. 3). If the interpretation that the slope projects to the composition of parent sulfate is correct, it is in accord with the widely accepted concept that aragonite preferentially precipitates at shallower depth than calcite. Our data set reinforces this concept by two lines of evidence. (1) The aragonite $^{87}\text{Sr}/^{86}\text{Sr}$ ratios are clustered around seawater ratios, whereas ratios of calcite deviate significantly from those of modern Gulf of Mexico seawater (Fig. 4), indicating formation of aragonite at or near to the seafloor while calcite formed at greater depth. (2) Aragonite has higher CAS contents than calcite (Table DR2), which is consistent with higher sulfate concentrations in pore fluids and formation at shallow sediment depth.

It has been suggested that CAS records the isotopic composition of sulfate of coeval seawater with no apparent fractionation for either oxygen or sulfur isotopes (e.g., Burdett et al., 1989; Lyons et al., 2004). Our data, however, suggest that CAS of diagenetic carbonates does not represent ambient seawater sulfate but in fact pore-water sulfate. Therefore, CAS in seep carbonate (this study) and diagenetic carbonate from organic matter-rich environments (Rennie and Turchyn, 2014) apparently reflect

changes in the pore-water concentration of sulfate whose stable isotope signatures have been altered to different degrees from those of coeval seawater sulfate in the course of sulfate-driven biogeochemical processes (Fig. DR2 in the Data Repository).

The inherent nature of seeps is that fluid flow intensity is highly variable both spatially and temporally. It was previously suggested that carbonate mineralogy and lipid biomarkers can be used to reconstruct seepage intensity (e.g., Peckmann et al., 2009; Haas et al., 2010; Nöthen and Kasten, 2011). However, because carbonate mineralogy and biomarkers are prone to diagenetic alteration (cf. Peckmann and Thiel, 2004), it will be difficult and sometimes impossible to use them in paleo-carbonate deposits to deduce paleo-seep intensity or geological SD-AOM processes in general. Our study now demonstrates that CAS in seep carbonates preserves the stable isotope signatures of sulfate over a spectrum of seep intensities.

Methane-rich environments are widely spread along continental margins in areas representing not only methane seeps but other organic matter-rich environments such as high-productivity and upwelling regions (e.g., Schulz, 2006). If authigenic carbonates occur in these environments, a large $\delta^{18}\text{O}/\delta^{34}\text{S}$ ratio (or slope) usually indicates an organic matter-sulfate coupled redox condition while a small slope indicates a methane-sulfate coupled redox condition. Thus, the new carbonate-based proxy can be used for the reconstruction of past depositional conditions. The new geological proxy successfully tested in this study provides a promising tool to reconstruct the activity and the spatial distribution of SD-AOM throughout most of Earth history.

CONCLUSIONS

Oxygen and sulfur isotope analyses of CAS in carbonates from three modern and two ancient methane-seep provinces revealed that CAS faithfully records the characteristic isotope fingerprint of SD-AOM, i.e., a small slope of the $\delta^{18}\text{O}_{\text{CAS}}/\delta^{34}\text{S}_{\text{CAS}}$ data array. The sulfate in seep carbonates originated from pore fluids rather than seawater. Depending on the flux of methane, the sulfate-methane transition zone is placed at different sediment depth. If SD-AOM occurs at shallow sediment depth in pore water of a seawater-like composition, a resulting small slope of $\delta^{18}\text{O}_{\text{SO}_4}$ - $\delta^{34}\text{S}_{\text{SO}_4}$ values lies on a line with the composition of coeval seawater sulfate. If SD-AOM occurs deeper in the sediment, an even smaller slope lies on a line with the composition of pore-water sulfate at the lower left end, corresponding to higher $\delta^{34}\text{S}$ and $\delta^{18}\text{O}$ values than those of seawater. Differences in the CAS patterns of aragonite and calcite from the Gulf of Mexico seep carbonates support this interpretation, revealing that the new proxy can also be used to reconstruct flow intensities and identify different redox environments at seeps or other sites where SD-AOM has occurred. Periods of enhanced methane flux may have occurred repeatedly in modern and ancient oceans. The new CAS stable isotope proxy will help to identify and better constrain SD-AOM activity throughout the geological record.

ACKNOWLEDGMENTS

Samples from the Gulf of Mexico were collected during projects funded by the U.S. Bureau of Ocean Energy Management and the U.S. National Oceanic and Atmospheric Administration's National Undersea Research Program. We thank editor James Schmitt, Sabine Kasten, and two anonymous reviewers for insightful comments on the manuscript. Funding was provided by the National Science Foundation of China (grants 41373085 and 41422602), the Hundred Talents Program of the Chinese Academy of Sciences to Feng, and partly from a U.S. National Science Foundation grant (EAR-1251824) to Bao.

REFERENCES CITED

- Aharon, P., and Fu, B.S., 2000, Microbial sulfate reduction rates and sulfur and oxygen isotope fractionations at oil and gas seeps in deepwater Gulf of Mexico: *Geochimica et Cosmochimica Acta*, v. 64, p. 233–246, doi:10.1016/S0016-7037(99)00292-6.
- Algeo, T.J., Luo, G.M., Song, H.Y., Lyons, T.W., and Canfield, D.E., 2015, Reconstruction of secular variation in seawater sulfate concentrations: *Biogeochemistry*, v. 12, p. 2131–2151, doi:10.5194/bg-12-2131-2015.

- Antler, G., Turchyn, A.V., Rennie, V., Herut, B., and Sivan, O., 2013, Coupled sulfur and oxygen isotope insight into bacterial sulfate reduction in the natural environment: *Geochimica et Cosmochimica Acta*, v. 118, p. 98–117, doi:10.1016/j.gca.2013.05.005.
- Antler, G., Turchyn, A.V., Herut, B., Davies, A., Rennie, V.C.F., and Sivan, O., 2014, Sulfur and oxygen isotope tracing of sulfate driven anaerobic methane oxidation in estuarine sediments: *Estuarine, Coastal and Shelf Science*, v. 142, p. 4–11, doi:10.1016/j.ecss.2014.03.001.
- Antler, G., Turchyn, A.V., Herut, B., and Sivan, O., 2015, A unique isotopic fingerprint of sulfate-driven anaerobic oxidation of methane: *Geology*, v. 43, p. 619–622, doi:10.1130/G36688.1.
- Boetius, A., and Wenzhöfer, F., 2013, Seafloor oxygen consumption fuelled by methane from cold seeps: *Nature Geoscience*, v. 6, p. 725–734, doi:10.1038/ngeo1926.
- Boetius, A., Ravensschlag, K., Schubert, C.J., Rickert, D., Widdel, F., Gieseke, A., Amann, R., Jørgensen, B.B., Witte, U., and Pfannkuche, O., 2000, A marine microbial consortium apparently mediating anaerobic oxidation of methane: *Nature*, v. 407, p. 623–626, doi:10.1038/35036572.
- Böttcher, M.E., and Parafiniuk, J., 1998, Methane-derived carbonates in a native sulfur deposit: Stable isotope and trace element discriminations related to the transformation of aragonite to calcite: *Isotopes in Environmental and Health Studies*, v. 34, p. 177–190, doi:10.1080/10256019708036345.
- Böttcher, M.E., Brumsack, H.J., and de Lange, G.J., 1998, Sulfate reduction and related stable isotope (^{34}S , ^{18}O) variations in interstitial waters from the eastern Mediterranean, in Robertson, A.H.F., et al., eds., *Proceedings of the Ocean Drilling Program, Scientific Results, Volume 160: College Station, Texas, Ocean Drilling Program*, p. 365–373, doi:10.2973/odp.proc.sr.160.002.1998.
- Böttcher, M.E., Thamdrup, B., and Vennemann, T.W., 2001, Oxygen and sulfur isotope fractionation during anaerobic bacterial disproportionation of elemental sulfur: *Geochimica et Cosmochimica Acta*, v. 65, p. 1601–1609, doi:10.1016/S0016-7037(00)00628-1.
- Bowles, M.W., Mogollon, J.M., Kasten, S., Zabel, M., and Hinrichs, K.-U., 2014, Global rates of marine sulfate reduction and implications for sub-sea-floor metabolic activities: *Science*, v. 344, p. 889–891, doi:10.1126/science.1249213.
- Bristow, T.F., and Grotzinger, J.P., 2013, Sulfate availability and the geological record of cold-seep deposits: *Geology*, v. 41, p. 811–814, doi:10.1130/G34265.1.
- Brunner, B., Bernasconi, S.M., Kleikemper, J., and Schroth, M.H., 2005, A model for oxygen and sulfur isotope fractionation in sulfate during bacterial sulfate reduction processes: *Geochimica et Cosmochimica Acta*, v. 69, p. 4773–4785, doi:10.1016/j.gca.2005.04.017.
- Burdett, J.W., Arthur, M.A., and Richardson, M., 1989, A Neogene seawater sulfur isotope age curve from calcareous pelagic microfossils: *Earth and Planetary Science Letters*, v. 94, p. 189–198, doi:10.1016/0012-821X(89)90138-6.
- Campbell, K.A., 2006, Hydrocarbon seep and hydrothermal vent paleoenvironments and paleontology: Past developments and future research directions: *Palaeogeography, Palaeoclimatology, Palaeoecology*, v. 232, p. 362–407, doi:10.1016/j.palaeo.2005.06.018.
- Deusner, C., Holler, T., Arnold, G.L., Bernasconi, S.M., Formolo, M.J., and Brunner, B., 2014, Sulfur and oxygen isotope fractionation during sulfate reduction coupled to anaerobic oxidation of methane is dependent on methane concentration: *Earth and Planetary Science Letters*, v. 399, p. 61–73, doi:10.1016/j.epsl.2014.04.047.
- Fritz, P., Basharmal, G.M., Drimmie, R.J., Ibsen, J., and Qureshi, R.M., 1989, Oxygen isotope exchange between sulfate and water during bacterial reduction of sulfate: *Chemical Geology*, v. 79, p. 99–105, doi:10.1016/0168-9622(89)90012-2.
- Fu, B., and Aharon, P., 1998, Sources of hydrocarbon-rich fluids advecting on the seafloor in the northern Gulf of Mexico: *Transactions of the Gulf Coast Association of Geological Societies*, v. 68, p. 73–82.
- Haas, A., Peckmann, J., Elvert, M., Sahling, H., and Bohrmann, G., 2010, Patterns of carbonate authigenesis at the Kouilou pockmarks on the Congo deep-sea fan: *Marine Geology*, v. 268, p. 129–136, doi:10.1016/j.margeo.2009.10.027.
- Johnston, D.T., Gill, B.C., Masterson, A., Beirne, E., Casciotti, K.L., Knapp, A.N., and Berelson, W., 2014, Placing an upper limit on cryptic marine sulphur cycling: *Nature*, v. 513, p. 530–533, doi:10.1038/nature13698.
- Joye, S.B., Boetius, A., Orcutt, B.N., Montoya, J.P., Schulz, H.N., Erickson, M.J., and Lugo, S.K., 2004, The anaerobic oxidation of methane and sulfate reduction in sediments from Gulf of Mexico cold seeps: *Chemical Geology*, v. 205, p. 219–238, doi:10.1016/j.chemgeo.2003.12.019.
- Knittel, K., and Boetius, A., 2009, Anaerobic oxidation of methane: Progress with an unknown process: *Annual Review of Microbiology*, v. 63, p. 311–334, doi:10.1146/annurev.micro.61.080706.093130.
- Luff, R., and Wallmann, K., 2003, Fluid flow, methane fluxes, carbonate precipitation and biogeochemical turnover in gas hydrate-bearing sediments at Hydrate Ridge, Cascadia Margin: Numerical modeling and mass balances: *Geochimica et Cosmochimica Acta*, v. 67, p. 3403–3421, doi:10.1016/S0016-7037(03)00127-3.
- Lyons, T.W., Walter, L.M., Gellatly, A.M., Martini, A.M., and Blake, R.E., 2004, Sites of anomalous organic remineralization in the carbonate sediments of South Florida, USA: The sulfur cycle and carbonate-associated sulfate, in Amend, J.P., et al., eds., *Sulfur Biogeochemistry: Past and Present: Geological Society of America Special Paper 379*, p.161–176, doi:10.1130/0-8137-2379-5.161.
- Niewöhner, C., Hensen, C., Kasten, S., Zabel, M., and Schulz, H.D., 1998, Deep sulfate reduction completely mediated by anaerobic methane oxidation in sediments of the upwelling area off Namibia: *Geochimica et Cosmochimica Acta*, v. 62, p. 455–464, doi:10.1016/S0016-7037(98)00055-6.
- Nöthen, K., and Kasten, S., 2011, Reconstructing changes in seep activity by means of pore water and solid phase Sr/Ca and Mg/Ca ratios in pockmark sediments of the Northern Congo Fan: *Marine Geology*, v. 287, p. 1–13, doi:10.1016/j.margeo.2011.06.008.
- Peckmann, J., and Thiel, V., 2004, Carbon cycling at ancient methane-seeps: *Chemical Geology*, v. 205, p. 443–467, doi:10.1016/j.chemgeo.2003.12.025.
- Peckmann, J., Birgel, D., and Kiel, S., 2009, Molecular fossils reveal fluid composition and flow intensity at a Cretaceous seep: *Geology*, v. 37, p. 847–850, doi:10.1130/G25658A.1.
- Rennie, V.C.F., and Turchyn, A.V., 2014, The preservation of $\delta^{34}\text{S}_{\text{SO}_4}$ and $\delta^{18}\text{O}_{\text{SO}_4}$ in carbonate-associated sulfate during marine diagenesis: A 25 Myr test case using marine sediments: *Earth and Planetary Science Letters*, v. 395, p. 13–23, doi:10.1016/j.epsl.2014.03.025.
- Schulz, H.D., 2006, Quantification of early diagenesis: Dissolved constituents in pore water and signals in the solid phase, in Schulz, H.D., and Zabel, M., eds., *Marine Geochemistry: Berlin-Heidelberg, Springer*, p. 73–124, doi:10.1007/3-540-32144-6_3.
- Staudt, W.J., and Schoonen, M.A.A., 1995, Sulfate incorporation into sedimentary carbonates, in Vairavamurthy, M.A., et al., eds., *Geochemical Transformations of Sedimentary Sulfur: American Chemical Society Symposium Series 612*, p. 332–345, doi:10.1021/bk-1995-0612.ch018.
- Torres, M.E., Bohrmann, G., Dube, T.E., and Poole, F.G., 2003, Formation of modern and Paleozoic stratiform barite at cold methane seeps on continental margins: *Geology*, v. 31, p. 897–900, doi:10.1130/G19652.1.
- Wankel, S.D., Bradley, A.S., Eldridge, D.L., and Johnston, D.T., 2014, Determination and application of the equilibrium oxygen isotope effect between water and sulfite: *Geochimica et Cosmochimica Acta*, v. 125, p. 694–711, doi:10.1016/j.gca.2013.08.039.
- Wortmann, U.G., and Paytan, A., 2012, Rapid variability of seawater chemistry over the past 130 million years: *Science*, v. 337, p. 334–336, doi:10.1126/science.1220656.
- Wortmann, U.G., Chernyavsky, B., Bernasconi, S.M., Brunner, B., Böttcher, M.E., and Swart, P.K., 2007, Oxygen isotope biogeochemistry of pore water sulfate in the deep biosphere: Dominance of isotope exchange reactions with ambient water during microbial sulfate reduction (ODP Site 1130): *Geochimica et Cosmochimica Acta*, v. 71, p. 4221–4232, doi:10.1016/j.gca.2007.06.033.

Manuscript received 14 June 2016
 Revised manuscript received 19 September 2016
 Manuscript accepted 19 September 2016

Printed in USA